Engenharia Agrícola

ISSN: 1809-4430 (on-line)

www.engenhariaagricola.org.br

Scientific Paper
Doi: http://dx.doi.org/10.1590/1809-4430-Eng.Agric.v44e20240054/2024

MODAL RESPONSE AND VIBRATION CHARACTERISTICS OF SUGAR BEET COMBINE HARVESTER FRAME

Jianguo Meng[1*], Zheng Li[1], Weidong Xian[1], Fangxu Li[1], Yanzhou Li[1]

[1*]Corresponding author. School of Mechanical Engineering, Inner Mongolia University of Science and Technology/Baotou, China.
E-mail: mjg101@163.com | ORCID ID: https://orcid.org/0000-0002-0385-1607

KEYWORDS

sugar beet harvester, frame, constrained modal, various operating conditions, modal response.

ABSTRACT

In complex environments, beet harvesters vibrate strongly under the influence of multiple sources of excitation. The modal constraints of the harvester's frame were obtained using modal simulation, and the accuracy of the finite element model was verified through SIMO modal testing. Additionally, field experiments were conducted to collect the vibration signals of the harvester under various conditions. Time-domain analysis revealed that the RMS value of the frame's Z-axis acceleration was highest in sugar beet fields and lowest on unpaved roads. There is a correlation between the operation of working components and changes in amplitude. Frequency domain analysis determined that the main vibration frequency of the frame was in the range of 0–75 Hz, and the operating frequency of the engine (35 Hz) and the power input shaft (12.7 Hz) excites the constrained modal of the frame, which may lead to resonance. Integrating the results of the modal response and vibration testing provides a more comprehensive approach to studying the vibration characteristics of agricultural machinery.

INTRODUCTION

Sugar beet is an important raw material for sugar production and a feed crop, and with the increased demand for sugar, the area of sugar beets planted in China has increased year by year (Finkenstadt, 2014). Sugar beet harvesting is highly seasonal, and the rapid temperature drop in autumn can result in a decrease in sugar content (Wang et al., 2021). Manual harvesting is labour-intensive, with long harvesting cycles, and sugar beets are prone to frostbite. Ensuring the long-term stability of the sugar beet harvester is important for guaranteeing the quality of the beet harvest (Yu et al., 2023). The beet harvester's field operations include excavation, conveying, sieving soil, loading, and other work (Pascuzzi et al., 2023), which will be simultaneously affected by the ground and the harvester's working parts, powered by the alternating load; the frame inevitably produces vibration (Wang et al., 2020). This will not only aggravate the vibration of the harvester frame but also accelerate the damage of the parts, reduce the working life of the harvester, and affect the driving safety and working efficiency (Bulgakov et al., 2017). According to statistics, 75% of structural fatigue failures are related to vibrations (An et al., 2020). This indicates that vibration is a key factor restricting sugar beet harvesters' reliability and driving comfort (Chen et al., 2020).

Many scholars have researched vibration in agricultural harvesters, mainly focusing on dynamic simulation analysis. They use modal analysis methods and vibration testing to study the mechanical vibration response and vibration reduction optimisation. Niu et al. (2022) proposed a method combining finite element simulation and vibration testing to obtain vibration frequencies that are beneficial for olive harvesting, aiming to improve the work efficiency of harvesters. Ali et al. (2021) collected the vibration signals of a cabbage harvester under off-road and field conditions, and analysed the vibration levels of the harvester under different operating conditions, providing a reference for the optimisation and improvement of the cabbage harvester. Wang et al. (2023) studied the vibration characteristics of a crawler pepper harvester under different operating conditions and the effects of various excitation sources on the chassis frame. Under field walking conditions, there were abnormal amplitudes in the left front of the chassis frame and the drive shaft of the cleaning and separating device, providing a reference for subsequent vibration

[1] School of Mechanical Engineering, Inner Mongolia University of Science and Technology/Baotou, China.

Area Editor: Fábio Lúcio Santos
Received in: 3-28-2024
Accepted in: 5-6-2024

reduction. Pang et al. (2019) established partial coherence functions for the vibration transmission of a harvester, and based on vibration testing, they analysed the main excitation sources of the combine harvester. Rubber sleeve nuts were designed to reduce the vibration transmitted from the cutter bar to the chute. Ma et al. (2020) conducted vibration testing on a crawler rape combine harvester to determine the key vibration excitation sources. Through single-factor experiments investigating the impact of the excitation frequency on the falling of siliques and seeds, it can be concluded that the reciprocating motion of the cutter bar would result in harvest losses. Ding et al. (2022) conducted vibration testing on the combine harvester under different feeding rates and studied the impact of crop feeding rate disturbances on the vibration mechanism of the entire harvester.

However, previous studies on the vibration response of agricultural machinery have focused on harvesting machines for stem crops (grains, rapeseed, peppers, etc.), while there is a lack of research on harvesting machines for root crops, which have more intense vibration and more complex excitation sources due to soil breaking and excavation. Moreover, there are few comprehensive analyses of the correspondence between vibration characteristics and modal shapes under different working conditions.

In order to determine the influencing factors of the vibration characteristics of the sugar beet combine harvester frame, the distribution law of the time-domain signals and the relationship between the frequency-domain signals and the excitation frequency of the working parts under different working conditions were investigated. In addition, through the constrained modal analysis of the harvester frame, the modal parameters of the frame were obtained. The intrinsic connection between the modal shape of the frame and the main vibration frequency was analysed, which provided a new direction for the study of the vibration characteristics of the root crop harvester under multi-source excitation. Additionally, it provided a data reference for the optimal design of the vibration reduction of the agricultural machinery.

MATERIAL AND METHODS

Structure of the Sugar Beet Combine Harvester

This paper focuses on a beet combine harvester (Gaofeng 4TL-4, Fengzhen Gaofeng Machinery Co., Ltd, Fengzhen City, Inner Mongolia Autonomous Region, China) whose structure is shown in Figure 1(a). The structure of the beet combine harvester includes an excavating device, conveying and separating devices, a vertical lifting device, a transverse loading device, an engine, a transmission system, walking wheels, etc. These components are multi-source exciters of the beet combine harvester. All working components are installed on the frame of the beet combine harvester. The frame is connected with walking wheels to support the conveying and separating devices, the vertical lifting device, the storage hopper, the hydraulic valve, and the transmission system.

The 4TL-4 beet harvester frame is made of hollow round tubes, rectangular steel tubes, and 8 mm steel plates welded together. The overall dimensions of the frame are 3540 mm × 2080 mm × 1095 mm (length × width × height). Finally, a 3D model of the beet harvester frame is completed using Solidworks 2021 (3D drawing software developed by French Dassault Systemes). This is shown in Figure 1(b).

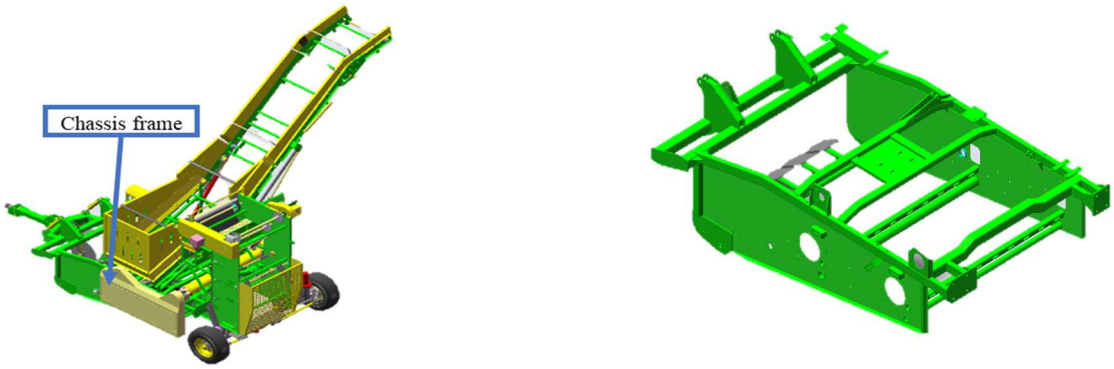

(a) Structure of sugar beet combine harvester

(b) Combine harvester chassis frame

FIGURE 1. Structure of a typical sugar beet combine harvester.

Modal Simulation

First, the 3D model of the beet harvester frame was imported into ANSYS Workbench for constrained modal analysis, and to improve the simulation speed, the frame model was simplified: 1) It was assumed that the material of the frame was isotropic, with a uniform density, and that the frame can be regarded as an integral whole. 2) The impact of welding on the vibration performance of the frame was neglected. 3) The structural features, such as assembly holes and chamfers, that do not significantly affect the stiffness of the frame were ignored. Before conducting the modal simulation, the frame material was set as Q235 structural steel. The relevant parameters of the material are shown in Table 1.

TABLE 1. Sugar beet harvester frame material parameters.

Density (kg/m^3)	Young's modulus (GPa)	Poisson's ratio	Yield strength (MPa)
7850	210	0.3	235

Based on the computer's performance and the size of the sugar beet harvester, the grid size was set to 10 mm, and automatic division was used to complete the frame meshing

and refine the local dimensions; 2937989 nodes and 1287990 cells were generated. The average quality of the mesh was 0.7782, and the mesh quality was good. After the pre-processing for modal analysis was completed, the first eight natural frequencies of the frame were solved, as shown in Figure 2.

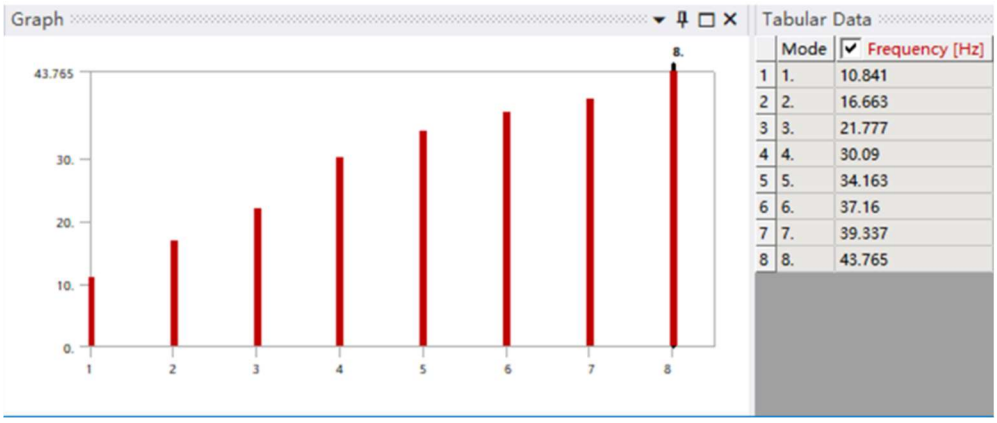

FIGURE 2. The first eight natural frequencies of the frame.

Modal Testing

The modal test simultaneously analyses the input and output signals to determine the modal natural characteristics of the frame. The experimental equipment includes the DH5902N dynamic signal acquisition instrument (produced by Jiangsu Donghua Testing Technology Co., Ltd.), the LC-04A force hammer, and three-direction acceleration sensors, as shown in Figure 3(a). The main performance parameters are shown in Table 2.

TABLE 2. Performance parameters of test instruments.

Instrument name	Performance index	Parameter values
DH5902N dynamic signal acquisition instrument	Channel	16
	Sampling bandwidth	100 kHz
	Degree of distortion	<0.5%
Three-direction acceleration sensors	Range	±500
	Frequency response	0.5~7 kHz
	Lateral sensitivity	<5%
LC-04A force hammer	Range	60 kN
	Accuracy	4 Pc/N

The experiment adopted the method of single input multiple output, and the excitation point was selected in the upper middle of the left wall panel of the frame to ensure that each measurement point could be successfully excited. The modal measurement point model of the frame was established in the DHDAS dynamic signal analysis system, as shown in Figure 3(b). The actual measurement point positions on the frame were numbered according to the measurement point model (Bhandari & Jotautienė, 2022).

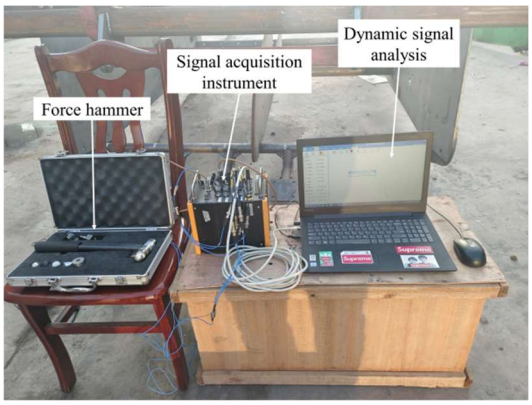

(a) Modal testing instrument

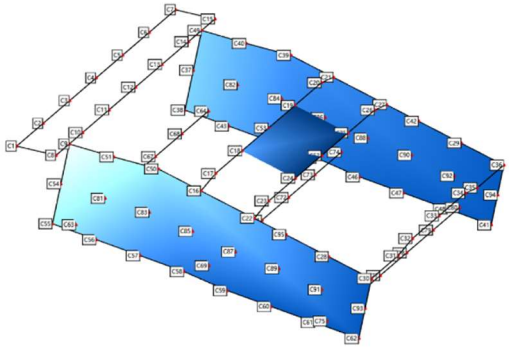

(b) Modal measurement point distribution

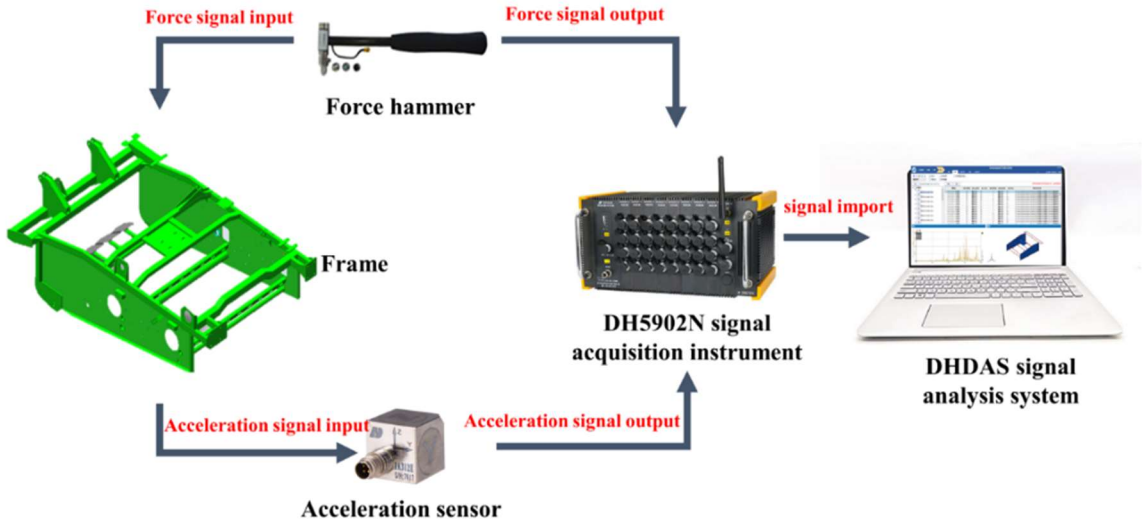

(C) Modal test schematic diagram

FIGURE 3. Modal test.

The force hammer and sensors were connected to the data acquisition instrument according to their numbers. During the experimental modal test, the excitation point on the beet harvester frame was struck with a force hammer, and the force hammer and the sensors transmitted the collected force and acceleration signals back to the dynamic signal analysis system to identify the first eight orders of the frame constrained modal. The modal test schematic diagram is shown in Figure 3(c).

Vibration Signal Acquisition

A vibration testing system that meets the requirements of the experiment was built; it includes the DH5902N dynamic signal acquisition instrument, three-direction acceleration sensors, and the DHDAS dynamic signal analysis system. In October 2023, field vibration tests were conducted in the sugar beet test field of Siziwang Banner, Inner Mongolia. The experimental site is shown in Figure 4.

(a) Sugar beet field

(b) Unpaved road

FIGURE 4. Harvester vibration tests under different working conditions.

The vibration signals of the sugar beet combine harvester were collected by acceleration sensors under three typical working conditions: idling, road transport, and field harvesting. The idle condition was divided into two situations: engine only and all parts working. The driving speed of the sugar beet harvester could be categorised into low (2.1 km/h), medium (2.6 km/h), and high (3.2 km/h) speeds. The testing scheme is shown in Table 3.

TABLE 3. Field vibration testing scheme.

Test numbers	Test conditions	Test environment	Running state	Vehicle speed (km/h)
1	Idle condition	Cement road	No load, static, engine only	0
2	Idle condition	Cement road	No load, static, all parts working	0
3	Transport condition	Unpaved road	No load, first gear, all parts working	2.1
4	Transport condition	Unpaved road	No load, second gear, all parts working	2.6
5	Transport condition	Unpaved road	No load, third gear, all parts working	3.2
6	Field condition	Sugar beet field	No load, second gear, all parts working	2.6
7	Field condition	Sugar beet field	Normal harvest, second gear, all parts working	2.6

* The working parts include digging devices, conveying and separating devices, vertical lifting devices, and other components.

The selected test points for the vibration test should be able to reflect the vibration of the machine and the local deformation of the larger position. The measurement points of the frame were the frame traction beam (measurement point 1), the reducer support beam (measurement point 2), the transverse conveyor support bracket (measurement point 3), the drive shaft bearing seat (measurement point 4), the power input shaft support (measurement point 5), and five other measurement points, and the distribution of the measurement points is shown in Figure 7. For the convenience of data processing, the X, Y, and Z channels of the acceleration sensor correspond to the vibration signals of the beet harvester in the longitudinal, transverse, and vertical directions, respectively. During the test, the sampling frequency was set to 1 kHz. The sampling time was 60 s and each test scheme was sampled three times (Harikrishnan & Gopi, 2017). The set of data with the best signal quality was analysed.

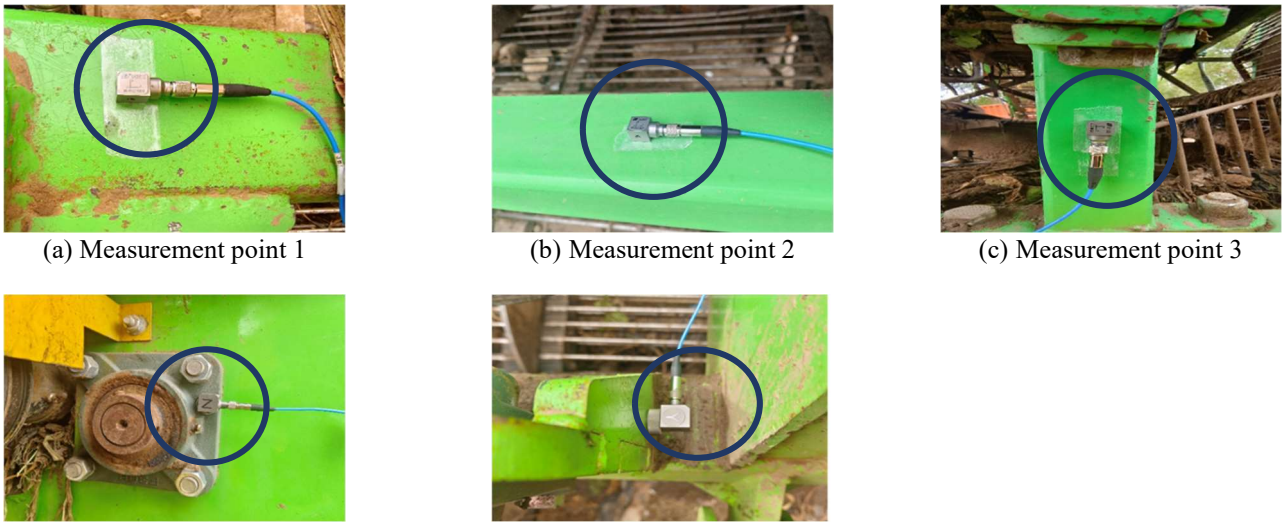

(a) Measurement point 1 (b) Measurement point 2 (c) Measurement point 3

(d) Measurement point 4 (e) Measurement point 5

FIGURE 5. Measurement point locations.

Post-processing of Vibration Signals

In the engineering field, the root mean square (RMS) value of acceleration is used to evaluate the impact of the vibration performance of agricultural equipment on structures. Generally, the larger the RMS value of acceleration, the more likely it is to cause structural damage and reduced driving comfort. The RMS value of acceleration can be expressed by Formula (1) (Gao et al., 2017):

$$RMS = \sqrt{\frac{1}{N}\sum_{i=1}^{N} x_i^{\,2}} = \sqrt{\frac{x_1^{\,2} + x_2^{\,2} + \cdots + x_n^{\,2}}{N}} \quad (1)$$

Where,

x_i is the real-time acceleration value (m/s^2);

N is the average number of times.

There is a correlation between the vibration acceleration in the three directions at each measurement point. To assess the overall effect of vibration, the RMS value of the total vibration acceleration at each measurement point in the Cartesian coordinate system can be expressed by Formula (2):

$$a_i = \sqrt{\frac{a_x^{\ 2} + a_y^{\ 2} + a_z^{\ 2}}{3}} \quad (2)$$

Where:

a_i is the RMS value of acceleration at the ith measurement point (m/s^2);

a_x, a_y, and a_z are the RMS values of acceleration at the measurement point in the X, Y, and Z directions (m/s^2).

In order to further study the frame's frequency-domain characteristics, the time-domain signals were transformed into frequency-domain signals through the fast Fourier transform (FFT). The Fourier transform can be described by Formula (3) (Wei et al., 2023):

$$X[k] = \sum_{n=0}^{N-1} x[n] e^{-i\frac{2\pi}{N}nk} \quad (3)$$

Where:

N is the number of collected signals;

$x[n]$ is the time;

e is the base of the natural logarithm;

i is the imaginary number.

Frame Vibration Source Analysis

The frame was subjected to vibration from the engine, transmission system, conveying and separating device, vertical lifting device road excitation, etc., and each source of vibration had its excitation frequency (Wang et al., 2019). When the excitation frequency and the natural frequencies of the structure satisfy Formula (4), the structure will undergo resonance:

$$0.75\omega_i \le \omega_j \le 1.3\omega_i \quad (4)$$

Where:

ω_i is the frame's natural frequency (Hz);

ω_j is the main working parts' excitation frequency (Hz).

In this study, the sugar beet harvester used a four-cylinder four-stroke diesel engine. The engine's explosive excitation frequency is shown in Formula (5) (Li et al., 2022):

$$f = \frac{2nz}{60\tau} \quad (5)$$

Where:

f is the engine's excitation frequency (Hz);

z is the number of engine cylinders (constant);

n is the engine's speed (r/min);

τ is the number of engine strokes (constant).

The engine was operating at 2100 r/min, and the excitation frequency of the engine was calculated to be 70 Hz. The rotational speeds of the main working parts of the beet harvester were measured using a contact tachometer, and the theoretical vibration frequencies of the working parts were calculated using Formula (6), as shown in Table 4:

$$f = \frac{n}{60} \quad (6)$$

Where:

f is the theoretical excitation frequencies of the working parts (Hz);

n is the rotational speed of the working parts (r/min).

In addition to the engine and the main working parts, there is also the excitation of the harvester by the road, and the road excitation frequency is in the low-frequency range of 0 to 2.4 Hz.

TABLE 4. The theoretical vibration frequency of the main excitation sources.

Main excitation source	Rpm (r/min)	Vibration frequency (Hz)
Engine	2100	70
Primary driving shaft	392	6.5
Secondary driving shaft	380	6.3
Primary seedling-pulling roller	506	8.4
Secondary seedling-pulling roller	152	2.5
Power input shaft	760	12.7

RESULTS AND DISCUSSION

Constrained Modal Analysis

The sugar beet combine harvester is a multi-degree-of-freedom elastic vibration system. During the harvesting operation of the harvester, multiple excitation forces act on the frame, causing a complex vibration response and frame deformation. The constrained modal shapes of the frame solved using ANSYS software are shown in Figure 6. The frequencies of the first eight constrained modals of the frame were concentrated in the range of 10.841–43.765 Hz, the frequency of the first torsional modal was 21.777 Hz, and the frequency of the first bending modal was 10.841 Hz; the linear combination of the bending and torsional modals constitutes the low-order vibration of the frame. From analysing the first eight orders of vibration modal shapes of the frame, it can be seen that the maximum amplitude of the frame appeared in the frame of the fifth order of the natural frequency 34.163 Hz, and its amplitude was 7.4026 mm. The amplitude of the next constrained modal frequencies of 37.16 Hz and 43.765 Hz was also relatively large, and the deformation was mainly manifested in the up-and-down oscillation of the excavation shovel along the Z-axis.

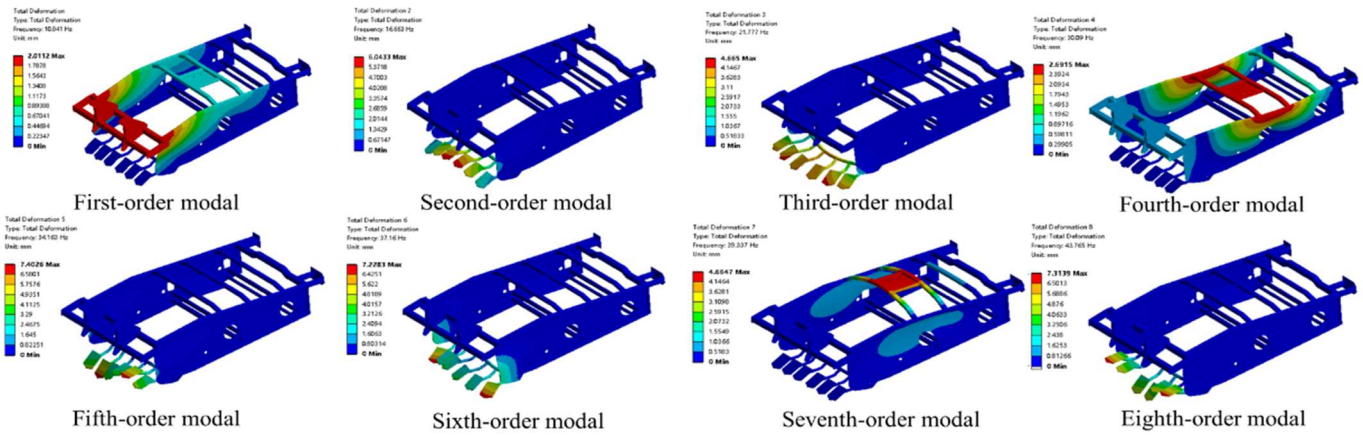

FIGURE 6. The finite element modal shapes of the chassis frame.

The response function of the frame model was calculated using the DHNAS dynamic signal analysis system to obtain the natural frequencies and modal shapes of the frame, and the results are shown in Figure 7. The frequencies of the first eight orders of the frame's constrained modal are concentrated between 9.848 and 43.494 Hz. The first-order frequency of the frame's constrained modal is 9.848 Hz, which is mainly due to the bending of the frame's wall panels at the front side. Similarly, it can be seen that the second to eighth frequencies of the frame-constrained modal are 15.694 Hz, 22.406 Hz, 29.993 Hz, 35.637 Hz, 37.245 Hz, 39.369 Hz, and 43.494 Hz, respectively. The frequencies of each order of the frame's modal and the corresponding damping ratios are shown in Table 5. The deformation of the frame mainly occurs at the two side wall panels, cross beams, and gearbox support beams, and the deformation in these parts will reduce the field operation efficiency of the sugar beet harvester.

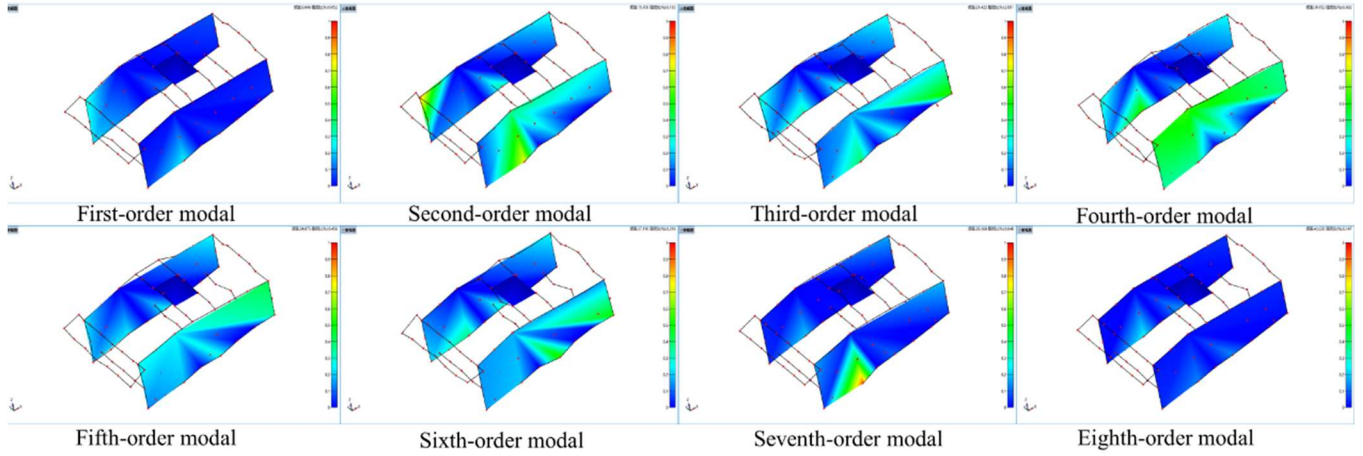

FIGURE 7. The experimental modal shapes of the chassis frame.

TABLE 5. The first eight experimental constrained modal values of the frame.

Orders	Modal frequency (Hz)	Damp ratio (%)
1	9.848	0.052
2	15.694	0.150
3	22.406	2.091
4	29.993	0.682
5	35.637	0.456
6	37.245	0.219
7	39.369	0.048
8	43.494	0.147

By using the modal assurance criterion (MAC) of frequency response function synthesis to verify the correlation of the experimental modal shapes, as shown in Figure 8, it can be seen that the modal shapes of each order are mutually orthogonal, and the MAC of modal shapes of different orders is 0, which indicates that the test can effectively identify the modal parameters (Mbarek et al., 2018).

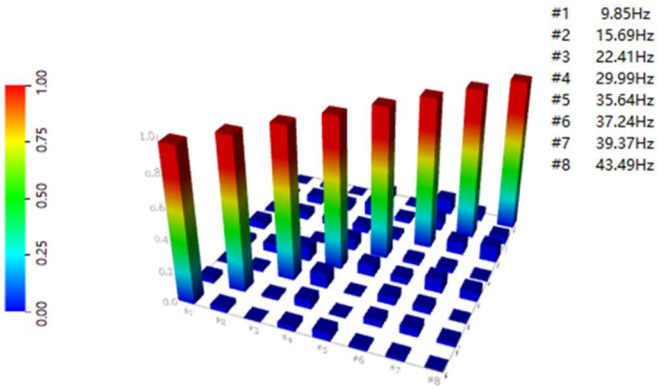

FIGURE 8. The MAC of the frame modal experiment.

Frame modal testing is an important step in verifying the accuracy of the results obtained from the finite element model. The comparison of the test results from the finite element modal and the experimental modal is shown in Figure 9. It can be seen from Figure 9 that the trends of the natural frequencies of the finite element modal and the experimental modal are consistent with each other, and the maximum error is 1.474 Hz. This indicates that the established finite element model is reliable and accurate, which is in line with the actual situation.

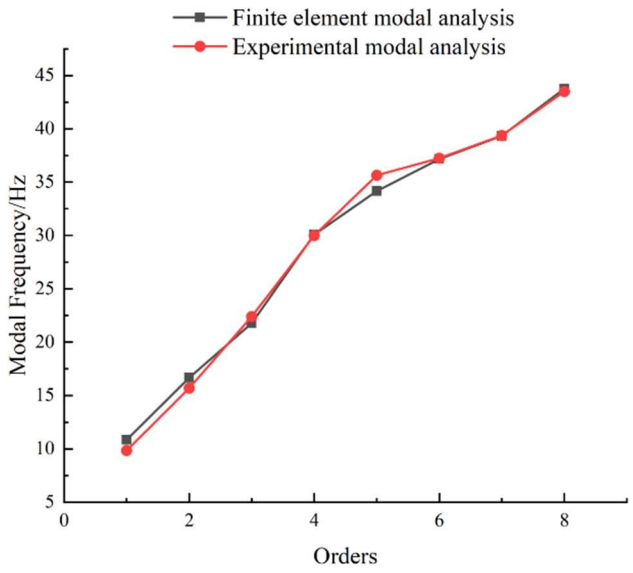

FIGURE 9. Comparison of the finite element modal and the experimental modal.

Time Domain Analysis

The accumulation of vibration energy in sugar beet harvesters in complex field environments can lead to the failure of the frame. The beet harvester completed the beet harvesting operation at a speed of 2.6 m/s under the harvesting condition. The time-domain signals in the three directions of each measurement point under harvesting conditions were obtained from the sensors, as shown in Figure 10. It is worth noting that the amplitude of the time-domain signals on the Z-axis exceeded the amplitude of the time-domain signals on the X-axis and Y-axis at all measurement points except for measurement points 3 and 5. This result means that most locations on the frame are subjected to greater vibration in the direction perpendicular to the ground. Therefore, subsequent harvester improvements should concentrate on the vibration characteristics in the Z-axis direction.

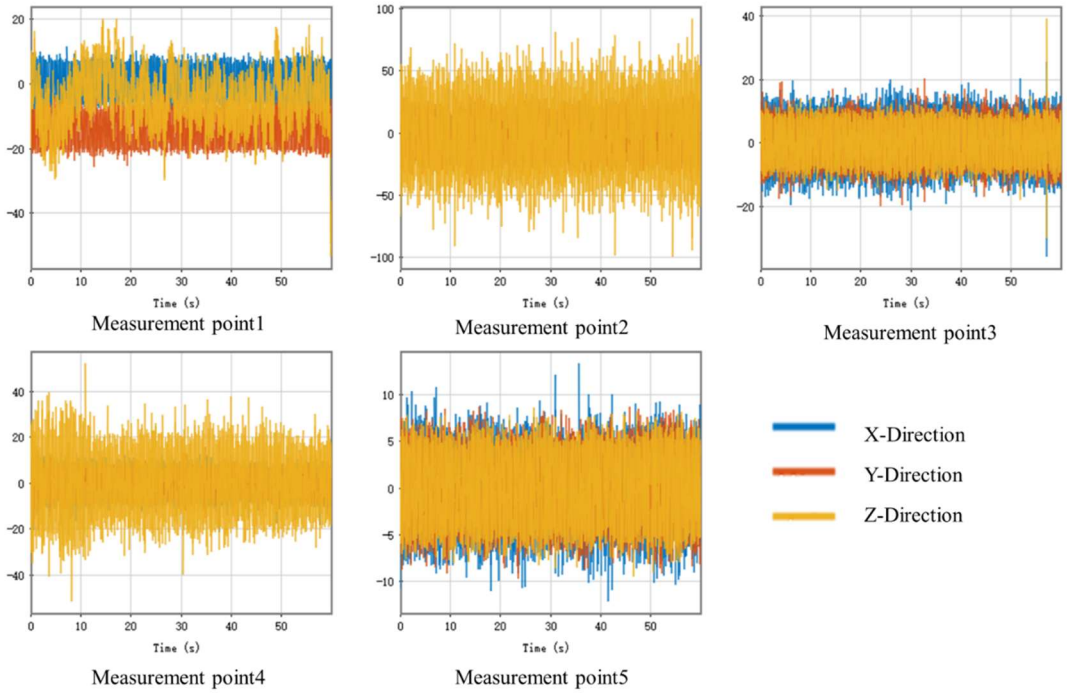

FIGURE 10. Time-domain signals at each measurement point in field conditions.

Time-domain analysis was conducted on the vibration signals under three different operating conditions: idle, road transportation, and field harvesting. The total vibration analysis diagram of each measuring point under different working conditions is shown in Figure 11(a). The vibration time-domain analysis diagrams of the frame during idle, road transport, and field harvesting conditions are shown in Figures 11(b), 11(c), and 11(d), respectively.

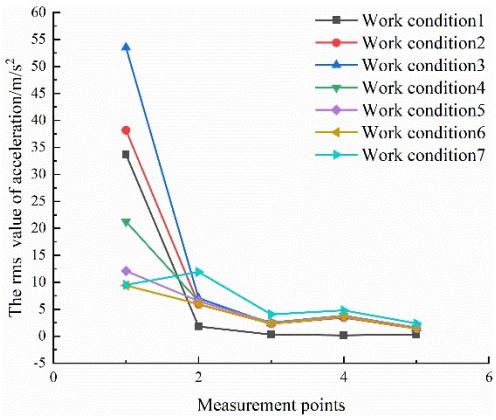

(a) Total vibration analysis diagram

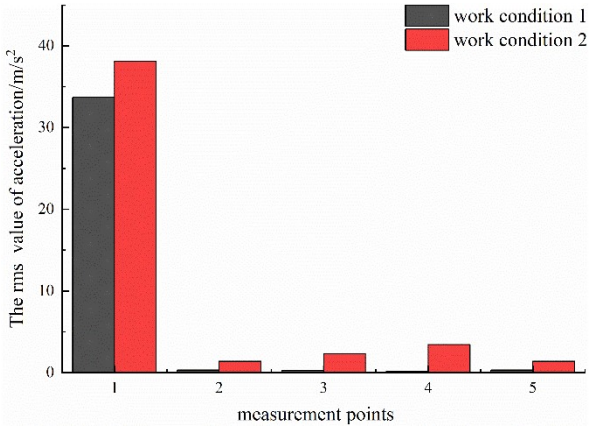

(b) Idle condition

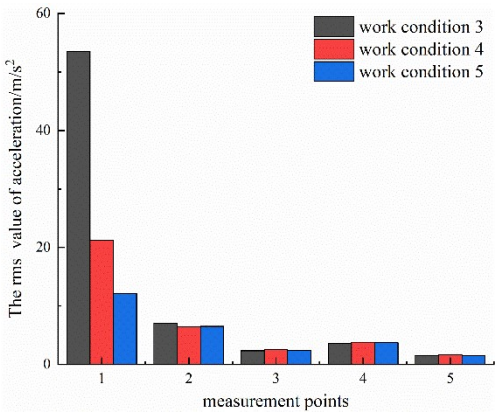

(c) Road transport condition

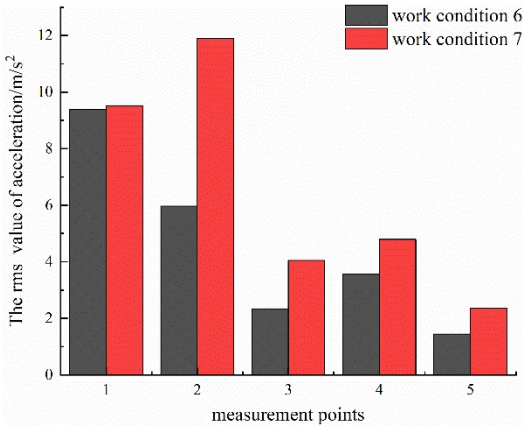

(d) Field harvesting condition

FIGURE 11. Root-mean-square (RMS) value of frame vibration acceleration.

It can be seen from Figure 11(a) that the amplitude was significantly higher at measurement point 1 than at the other measurement points, and the RMS of acceleration at the other measurement points was smaller, which might be caused by the higher centre of gravity of the frame traction beam (measurement point 1). The vibration characteristics of the frame under various working conditions were summarised, and measurement points 1, 2, and 4 were located in the middle and front positions of the frame, which had higher RMS values. Measurement points 3 and 5 were located in the rear of the frame, which had lower RMS values. This indicates that the frame vibration is most affected by the engine, followed by the drive shaft, and lastly, the seedling-pulling roller; the vibration of the frame is mainly in the middle and front part of the frame, and the total amount of vibration of the beet harvester under the field conditions is greater than that of the other working conditions.

As shown in Figure 11(b), comparing working conditions 1 and 2, the total vibration level at various measurement points on the frame significantly increases when all working parts are operational. The vibration levels at the frame traction beam (measurement point 1), the reducer support beam (measurement point 2), the lateral conveyor support bracket (measurement point 3), the bearing seat of the drive shaft (measurement point 4), and the power input shaft support (measurement point 5) increase by 0.13, 2.26, 6.78, 19.5, and 3.34 times, respectively. This indicates that the operation of working parts has a significant impact on the vibration stability of the frame.

As shown in Figure 11(c), comparing working conditions 3, 4, and 5, the sugar beet harvester travels at low, medium, and high speeds. The total vibration level at each measurement point shows little variation (within a range of 10%), and it is even observed that the vibration amplitude is slightly smaller when the harvester is travelling at a high speed (3.6 m/s) compared to when it is travelling at a low speed (2.1 m/s). This indicates that changing the travel speed has a minimal impact on the vibration reliability of the frame. Maintaining a suitable travelling speed can effectively reduce the influence of the travelling speed on the vibration of the whole machine.

As shown in Figure 11(d), a comparison was made between working conditions 6 and 7. When sugar beets enter the harvester, except for measurement point 1, the total vibration levels at other measurement points significantly increased, with increases of 1.3%, 99.6%, 72.7%, 34.3%, and 64%, respectively. This indicates that the entry of sugar beets has a significant impact on the vibration stability of the frame. This is because the entry of sugar beets, soil, and other mixtures into the harvester causes fluctuations in the loads of various working components, thereby intensifying the vibrations of the frame.

Frequency Domain Analysis

Whole-machine vibrations are often caused by low-frequency vibrations, while high-frequency vibrations are usually far from the structural natural frequencies and have smaller amplitudes (Castro-Garcia et al., 2018). Therefore, the focus is on the low-frequency vibration characteristics that affect the fatigue damage of the frame. The Fourier transform of the acceleration signal, when the combine harvester was in working condition 7 (field harvesting operation), was calculated to obtain the vibration main frequencies of the first three orders and the amplitude of five measurement points to show the frequency domain characteristics, as shown in Table 6.

TABLE 6. Main frequency and peak amplitude of each measurement point.

Test point	Order	X direction		Y direction		Z direction	
		Frequency (Hz)	Amplitude ($m \cdot s^{-2}$)	Frequency (Hz)	Amplitude ($m \cdot s^{-2}$)	Frequency (Hz)	Amplitude ($m \cdot s^{-2}$)
1	1	12.70	1.47	12.70	1.06	11.72	0.97
	2	17.58	0.37	70.31	0.76	35.16	0.62
	3	57.62	0.35	35.16	0.48	3.91	0.78
2	1	12.70	0.82	12.70	0.73	70.31	1.52
	2	35.16	0.74	25.39	0.68	68.36	1.43
	3	25.39	0.73	70.31	0.65	25.39	1.22
3	1	70.31	1.37	12.70	1.16	70.31	0.83
	2	75.20	1.29	70.31	0.90	75.20	0.62
	3	35.16	0.89	75.20	0.45	66.41	0.40
4	1	12.70	0.96	35.16	0.95	12.70	1.90
	2	78.13	0.46	11.72	0.36	36.13	0.84
	3	31.25	0.42	75.20	0.32	38.09	0.69
5	1	35.16	0.68	11.72	0.54	12.70	1.53
	2	12.70	0.62	75.20	0.51	48.83	0.36
	3	92.77	0.60	35.16	0.50	10.74	0.28

The arrangement of measurement points was related to the location of the vibration source. Measurement points 1 and 5 were located at the front of the frame (near the engine) to assess the effect of the engine on the frame. Measurement points 2 and 3 were located in the middle of the frame (near the transverse conveyor) to assess the effect of the transverse conveyor on the frame. Measurement point 4 was utilised to estimate the effect of the drive shaft on the frame. From Table 6, the following conclusions can be drawn:

(1) The vibration amplitudes in the X, Y, and Z directions of the sugar beet harvester reach their maximum values at the frame traction beam (measurement point 1), the transverse conveyor support bracket (measurement point 3), and the drive shaft bearing seat (measurement point 4). The maximum vibration amplitudes were measured as 1.47 m/s² (12.70 Hz), 1.16 m/s² (12.70 Hz), and 1.90 m/s² (12.70 Hz), respectively. The maximum peak frequency appeared around 12.70 Hz, which closely corresponds to the excitation frequency of the power input shaft. The major frequencies of 25.39 Hz and 75.20 Hz at measurement points 2 and 3, which are not within the excitation range of the six excitation sources (shown in Table 4), indicate the formation of 25.39 Hz and 75.20 Hz coupling frequencies.

(2) The main vibration frequencies of different measurement points of the frame were analysed; frequencies of 12.70 Hz (close to the working frequency of the power input shaft and the frequency-multiplied components of the drive shaft), 35.16 Hz (close to the engine's frequency division) and 70.31 Hz (close to the working frequency of the engine) all existed, which indicates that the engine and the power input shaft were the main excitation sources causing the vibration of the frame, while the excitation frequency of the seedling-pulling rollers contributed very little to the vibration of the frame of the sugar beet harvester.

Due to the differences in the terrain and travelling speeds, there were significant differences in the distribution of the main frequencies and peaks of the same measurement point observed under three typical operating conditions: idling, road transport, and field harvesting. Figure 12 shows the frequency domain curves at different measurement point locations in the frame under field harvesting conditions.

These figures highlight the significance of the operating frequency close to the power input shaft and the frequency-multiplied components of the conveyor chain drive shaft in the frequency-domain curves. The second most significant frequency comes from the engine operating frequency. It is worth noting that the frequency and peak distributions of the sugar beet harvester differ significantly at different measurement points. For example, measurement point 3 (transverse conveyor support bracket) and measurement point 4 (drive shaft bearing seat) exhibit lower peaks at 35.16 Hz (close to the engine's frequency division) and 70.31 Hz (close to the operating frequency of the engine) compared to the other measurement point locations. Measurement points 3 and 4 are located in the middle and rear of the frame and are less affected by engine excitation. When the vibration frequency was 12.70 Hz, the amplitude of the frame traction beam (measurement point 1) exceeded 1 m/s² in the X, Y, and Z directions, which indicates that the frame tractor beam may have local resonance; this coincides with the fatigue damage of the frame tractor beam in the actual use of this type of beet harvester. In the design, vibration isolation measures should be added between the engine, drive train, and frame, and the local modal of the frame should be changed to avoid local resonance.

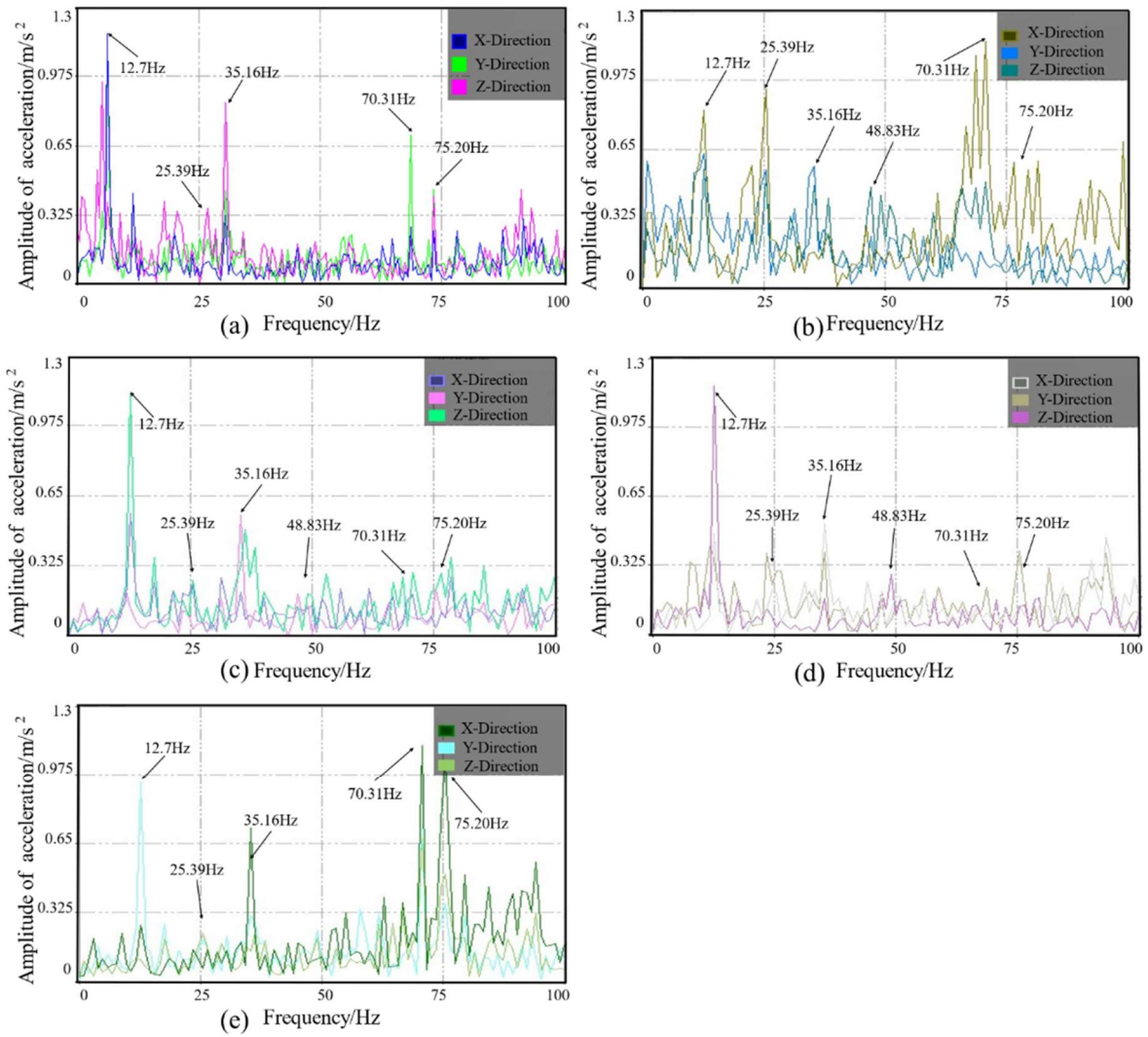

FIGURE 12. Frequency-domain curves of different measurement points in field conditions: (a) Measurement point 1; (b) measurement point 2; (c) measurement point 3; (d) measurement point 4; (e) measurement point 5.

Modal Response of Sugar Beet Harvester Frame under Multiple Excitations

The main working parts on a combine harvester can excite the modal vibration response of a sugar beet harvester frame, as shown in Table 4. When the vibration frequency reaches a specific value, a certain order of modal shapes of the frame can be excited and a specific deformation of the frame can occur. The vibration deformation law of the frame can be revealed by analysing the correspondence between the modal results and the vibration frequency of the harvester frame, as shown in Figure 13.

As shown in Figure 13, under the field harvesting condition, the vibration frequency of the power input shaft and the second doubling frequency of the seedling-pulling rollers (12.70 Hz, 11.72 Hz) will stimulate the first-order modal (local modal) of the beet harvester, which will increase the vibration of the frame traction beam and cause fatigue damage. The engine's frequency division (36.15 Hz, 31.25 Hz) will excite the fifth-order modal (local modal) and the fourth-order modal, which will cause the middle and upper bending deformation of the harvester frame and the local deformation of the front wall panels. In addition, the sugar beet combine harvester operation process is accompanied by multiple sources of vibration, as well as road excitation; many of these sources are in the range of the first eight orders of the natural frequency, easily resulting in the complex coupled vibration and resonance of the frame. If the vibration response of the sugar beet combine harvester is to be reduced, the overlap between the excitation frequencies of the working parts and the constrained modal frequencies of the frame should be reduced. By optimising the frame structure, the combine harvester frame-constrained frequency can be varied to stagger the excitation frequencies from the multi-source excitation. It is also possible to reduce frame vibration by changing the excitation frequencies of the main working parts.

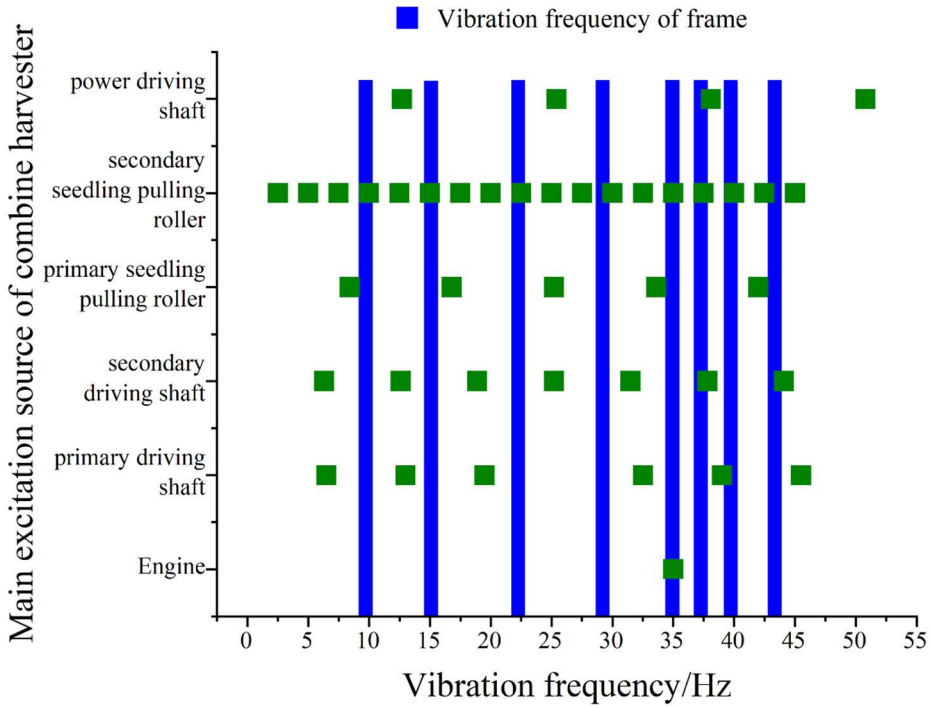

FIGURE 13. Frame vibration response under multi-source excitation.

CONCLUSIONS

In this study, a 4TL-4 sugar beet harvester is taken as the research object, and its vibration characteristics under different working conditions are investigated based on the modal. The conclusions of this paper are as follows:

(1) The intrinsic properties of the finite element modal and the experimental modal were almost the same, and the accuracy of the modal simulation was verified by using the modal test. The first eight constrained modal frequencies of the frame range from 10.841 to 43.765 Hz. The modal shapes of the sugar beet harvester frame were primarily bending and twisting shapes, with local modals also present. In addition, the engine's frequency division (35 Hz), the frequency-multiplied components (13 Hz, 12.6 Hz) of the drive shaft, and the working frequency (12.70 Hz) of the power input shaft were all within the frequency range of the first eight constrained modals, which may cause the vibration coupling and resonance of the frame.

(2) The time-domain analysis indicates that among the three-axis accelerations measured at five points on the frame, the time-domain signal amplitude of the Z-axis exceeds those of the X-axis and Y-axis. The RMS values at measurement points 1, 2, and 4 exceed those at measurement points 3 and 5, indicating that frame vibration mainly occurs in the middle front part of the frame, with the engine having the greatest impact on frame vibration. It is worth noting that as the sugar beet enters the harvester, the RMS values of the frame's acceleration also increase. A comprehensive analysis shows that the vibration acceleration under field conditions is the highest, followed by transport conditions, and the vibration acceleration under idle conditions is the lowest. This indicates that the operation of various components has a significant impact on the stability of frame vibration.

(3) Frequency domain analysis indicates that the operating frequencies of the harvester mainly fall within the range of 0 to 80 Hz. Under field harvesting conditions, the primary influencing factors of frame vibration are the engine's frequency division (35 Hz) and the operating frequency of the power input shaft (12.7 Hz). The main excitation sources causing frame vibration include the engine and transmission system, while the contribution of the seedling-pumping roller was small. The main vibration frequencies of 25.39 Hz and 75.20 Hz are not within the excitation range of the excitation sources, indicating the formation of coupled frequencies.

(4) By considering the results of modal analysis and vibration testing, the corresponding relationship between frame vibration frequencies and modal shapes was determined. Under the field harvesting condition, the theoretical frequency of the power driving shaft (12.7 Hz) was close to the first-order constrained modal of the frame, the doubled frequency of the seedling-pulling roller (16.8 Hz) was close to the second-order constrained modal of the frame, and the engine's frequency division (35 Hz) was close to the fifth-order constrained local modal of the frame, confirming the existence of resonance in the frame when the harvester was operating in the field.

This study comprehensively analyses modal responses and vibration characteristics, enabling the localization of maximum vibrations in harvesters and the estimation of potential deformations under complex excitation environments. It provides a more comprehensive approach to researching the vibration characteristics of agricultural machinery and serves as a theoretical reference for further vibration reduction optimization.

ACKNOWLEDGMENTS

The authors would like to gratefully acknowledge the Inner Mongolia Autonomous Region Key R&D and Achievement Transformation Programme Project (Grant No. 2022YFHH0122). Finally, the authors would like to thank the editors and reviewers for their valuable comments and constructive suggestions.

REFERENCES

Ali M, Lee YS, Chowdhury M (2021) Analysis of driving stability and vibration of a 20-kw self-propelled 1-row chinese cabbage harvester. Journal of Biosystems Engineering 46: 48-59. https://doi.org/10.1007/s42853-021-00087-w

An X, Li ZG, Zude-Sasse M, Tchuenbou-Magaia F, Yang YG (2020) Characterization of textural failure mechanics of strawberry fruit. Journal of Food Engineering 282: 110016. https://doi.org/10.1016/j.jfoodeng.2020.110016

Bhandari S, Jotautienė E (2022) Vibration analysis of a roller bearing condition used in a tangential threshing drum of a combine harvester for the smooth and continuous performance of agricultural crop harvesting. Agriculture 12(11): 1969. https://doi.org/10.3390/agriculture12111969

Bulgakov V, Adamchuk V, Nozdrovický L, Ihnatiev Y (2017) Theory of vibrations of sugar beet leaf harvesterfront-mounted on universal tractor. Acta Technologica Agriculturae 20(4): 96-103. https://doi.org/10.1515/ata-2017-0019

Castro-Garcia S, Sola-Guirado RR, Gil-Ribes JA (2018) Vibration analysis of the fruit detachment process in late-season 'Valencia'orange with canopy shaker technology. Biosystems Engineering 170: 130-137. https://doi.org/10.1016/j.biosystemseng.2018.04.007

Chen SR, Zhou YP, Tang Z, Lu SN (2020) Modal vibration response of rice combine harvester frame under multi-source excitation. Biosystems Engineering 194: 177-195. https://doi.org/10.1016/j.biosystemseng.2020.04.002

Ding HT, Chen SR, Zhou WW, Liang RZ (2022) Mechanism analysis of combine harvester's vibration characteristics under feeding interference. Transactions of the Chinese Society of Agricultural Machinery 53(S2): 20–27. https://doi.org/10.6041/j.issn.1000-1298.2022.S2.003

Finkenstadt VL (2014) A review on the complete utilization of the sugarbeet. Sugar Technology 16: 339-346. https://doi.org/10.1007/s12355-013-0285-y

Gao ZP, Xu LZ, Li YM, Wang YD, Sun PP (2017) Vibration measure and analysis of crawler-type rice and wheat combine harvester in field harvesting condition. Transactions of the Chinese Society of Agricultural Engineering 33(20): 48-55. https://doi.org/10.11975/j.issn.1002-6819.2017.20.006

Harikrishnan PM, Gopi VP (2017) Vehicle vibration signal processing for road surface monitoring. IEEE Sensors Journal 17(16): 5192-5197. https://doi.org/10.1109/JSEN.2017.2719865

Li X, Xu YX, Li NP, Yang B, Lei YG (2022) Remaining useful life prediction with partial sensor malfunctionsusing deep adversarial networks. IEEE/CAA Journal of Automatica Sinica 10(1): 121-134. https://doi.org/10.1109/JAS.2022.105935

Ma LN, Wei JY, Huang XM, Zong WY, Zhan GC (2020) Analysis of harvesting losses of rapeseed caused by vibration of combine harvester header during field operation. Transactions of the Chinese Society for Agricultural Machinery 51(S2): 134-138. https://doi.org/10.6041/j.issn.1000-1298.2020.S2.016

Mbarek A, Del Rincon AF, Hammami A, Iglesias M, Chaari F, Viadero F, Haddar M (2018) Comparison of experimental and operational modal analysis on a back to back planetary gear. Mechanism and Machine Theory 124:226-247. https://doi.org/10.1016/j.mechmachtheory.2018.03.005

Niu ZJ, Xu Z, Deng JT, Zhang J, Pan SJ, Mu HT (2022) Optimal vibration parameters for olive harvesting from finite element analysis and vibration tests. Biosystems Engineering 215: 228-238. https://doi.org/10.1016/j.biosystemseng.2022.01.002

Pang J, Li YM, Ji JT, Xu LZ (2019) Vibration excitation identification and control of the cutter of a combine harvester using triaxial accelerometers and partial coherence sorting. Biosystems Engineering 185: 25-34. https://doi.org/10.1016/j.biosystemseng.2019.02.013

Pascuzzi S, Bulgakov V, Adamchuk V, Holovach I, Nadykto V, Budzanivskyi M (2023) Study of the movement dynamics of a beet leaves harvester. Applied Sciences 13(2):841. https://doi.org/10.3390/app13020841

Wang FY, Zhang Q, Zhang ZY, Huang XP (2021) Development of comb type leaves clearing and top cutting machine for beets. Transactions of the Chinese Society of Agricultural Engineering (Transactions of the CSAE) 37(4): 69-79. https://doi.org/10.11975/j.issn.1002-6819.2021.4.009

Wang JW, Bai HC, Sun XB, Wang JL, Tang H, Zhou WQ (2019) Design and dynamic analysis of spray device for paddy field sprayer. Transactions of the Chinese Society for Agricultural Machinery 50(3): 69-79. https://doi.org/10.6041/j.issn.1000-1298.2019.03.007

Wang QS, Zhou JS, Gong D, Wang TF, Chen JX, YouTW, Zhang ZF (2020) The influence of the motor traction vibration on fatigue life of the bogie frame of the metro vehicle. Shock and Vibration 2020: 1-11. https://doi.org/10.1155/2020/7385861

Wang XJ, Cao YH, Fang WQ, Sheng HR (2023) Vibration Test and Analysis of Crawler Pepper Harvester under Multiple Working Conditions. Sustainability 15(10): 8112. https://doi.org/10.3390/su15108112

Wei ZJ, Gao QM, Xiang H, Xu P, Zhao PF (2023) Finite element analysis of the design of a mounted implement of fertilizer spreader based on HyperWorks. Journal of Guangxi University of Science and Technology 34(04): 17-24 https://doi.org/10.16375/j.cnki.cn45-1395/t.2023.04.003

Yu DY, He JF, Peng FH, Qian C, Zang Y, Zhang M H, Yang WW, Zeng GX, Chen JP, Qin W (2023) Study on Vibration Characteristics of Paddy Power Chassis under Different Driving Conditions Agriculture 13 (9): 1842. https://doi.org/10.3390/agriculture13091842